0026-895X/07/7105-1288–1297$20.00
MOLECULAR PHARMACOLOGY
Copyright © 2007 The American Society for Pharmacology and Experimental Therapeutics
Mol Pharmacol 71:1288–1297, 2007

Vol. 71, No. 5
33233/3202008
Printed in U.S.A.

Analogs of Methyllycaconitine as Novel Noncompetitive Inhibitors of Nicotinic Receptors: Pharmacological Characterization, Computational Modeling, and Pharmacophore Development

Dennis B. McKay, Cheng Chang, Tatiana F. González-Cestari, Susan B. McKay, Raed A. El-Hajj, Darrell L. Bryant, Michael X. Zhu, Peter W. Swaan, Kristjan M. Arason, Aravinda B. Pulipaka, Crina M. Orac, and Stephen C. Bergmeier

Division of Pharmacology, College of Pharmacy (D.B.M., T.F.G.-C., S.B.M., R.A.E., D.L.B.) and Department of Neuroscience, College of Medicine (M.X.Z.), The Ohio State University, Columbus, Ohio; Department of Pharmaceutical Sciences, School of Pharmacy, University of Maryland, Baltimore, Maryland (C.C., P.W.S.); and Department of Chemistry and Biochemistry, Ohio University, Athens, Ohio (K.M.A., A.P.B., C.M.O., S.C.B.)

Received December 13, 2006; accepted February 16, 2007

ABSTRACT

As a novel approach to drug discovery involving neuronal nicotinic acetylcholine receptors (nAChRs), our laboratory targeted nonagonist binding sites (i.e., noncompetitive binding sites, negative allosteric binding sites) located on nAChRs. Cultured bovine adrenal cells were used as neuronal models to investigate interactions of 67 analogs of methyllycaconitine (MLA) on native $\alpha 3\beta 4^*$ nAChRs. The availability of large numbers of structurally related molecules presents a unique opportunity for the development of pharmacophore models for noncompetitive binding sites. Our MLA analogs inhibited nicotine-mediated functional activation of both native and recombinant $\alpha 3\beta 4^*$ nAChRs with a wide range of IC_{50} values (0.9–115 μM). These analogs had little or no inhibitory effects on agonist binding to native or recombinant nAChRs, supporting noncompetitive inhibitory activity. Based on these data, two highly predictive 3D quantitative structure-activity relationship (comparative molecular field analysis and comparative molecular similarity index analysis) models were generated. These computational models were successfully validated and provided insights into the molecular interactions of MLA analogs with nAChRs. In addition, a pharmacophore model was constructed to analyze and visualize the binding requirements to the analog binding site. The pharmacophore model was subsequently applied to search structurally diverse molecular databases to prospectively identify novel inhibitors. The rapid identification of eight molecules from database mining and our successful demonstration of in vitro inhibitory activity support the utility of these computational models as novel tools for the efficient retrieval of inhibitors. These results demonstrate the effectiveness of computational modeling and pharmacophore development, which may lead to the identification of new therapeutic drugs that target novel sites on nAChRs.

The physiological roles of neuronal nicotinic acetylcholine receptors (nAChRs) in synaptic release of acetylcholine and their involvement in the modulation of other important neurotransmitters such as norepinephrine, serotonin, GABA, glutamate, and dopamine make nAChRs prime targets for therapeutic interventions. In addition, nAChRs have been linked to pain, epilepsy, and many neurodegenerative diseases, such as Alzheimer's disease and Parkinson's disease, and psychiatric disorders, such as depression and schizophrenia. The development of new drugs to target these receptors has been slow for several reasons: 1) multiple subtypes of nAChRs are expressed in the central and peripheral nervous systems; 2) few drugs are available that selectively target nAChR subtypes; and 3) information on the physiological roles of specific nAChR subtypes is limited. A key approach to provide a better understanding of physiological processes and pathophysiological conditions involving

This project was supported by National Institutes of Health grants DA12707 (to S.C.B. and D.B.M.) and DA10569 (to D.B.M.). D.L.B. was supported as a National Institute on Drug Abuse Underrepresented Minority Supplement Awardee (DA10569).

Article, publication date, and citation information can be found at http://molpharm.aspetjournals.org.

doi:10.1124/mol.106.033233.

ABBREVIATIONS: nAChR, neuronal nicotinic acetylcholine receptor; MLA, methyllycaconitine; QSAR, quantitative structure-activity relationship; CoMFA, comparative molecular field analysis; CoMSIA, comparative molecular similarity index analysis; GASP, genetic algorithm similarity program; PRESS, predictive error sum of squares; HBA, hydrogen-bond acceptor.

nAChRs is the identification and development of small molecules that selectively interact with specific nAChR subtypes.

A variety of agents have been found in nature that interact with nAChRs (Daly, 2005), some of which are used to pharmacologically differentiate nAChR subtypes, including snake venom neurotoxins (Luetje et al., 1990) and marine snail conotoxins (Livett et al., 2004). However, a problem associated with the therapeutic usefulness of these molecules is that they are proteins. The plant alkaloid methyllycaconitine (MLA) is a hexacyclic norditerpenoid with a well-documented high-affinity, competitive antagonism for $\alpha7$ nAChRs (Ward et al., 1990). However, MLA also acts as a competitive antagonist on other nAChR subtypes, including $\alpha3\beta4$ nAChRs (Bryant et al., 2002; Free et al., 2002, 2003) and $\alpha4\beta2$ nAChRs (Yum et al., 1996), albeit with lower affinity. This activity of MLA on multiple neuronal nAChR subtypes suggests that MLA analogs could be used to elucidate structural determinants important for activity on specific nAChR subtypes.

Taking this approach, our laboratory (Bergmeier et al., 1999, 2004; Bryant et al., 2002) and others (Goodall et al., 2005) have synthesized analogs of MLA. Our laboratory has reported that these analogs seem to act as noncompetitive inhibitors of $\alpha3\beta4$* nAChRs based on their ability to inhibit nAChR-mediated neurosecretion without inhibition of agonist binding to nAChRs (Bergmeier et al., 1999, 2004; Bryant et al., 2002). In addition, these analogs had no effects on agonist binding to $\alpha4\beta2$ and $\alpha7$ nAChRs (Bergmeier et al., 1999, 2004; Bryant et al., 2002). Similar findings have recently been reported by Barker and associates (2005) with a tricyclic analog of MLA. We now report on the pharmacological activities of 67 MLA analogs on functional activation of native and recombinant nicotinic receptors. Our hypotheses are that these pharmacological studies, using such large numbers of structurally similar compounds, can be used to generate predictive 3D-QSAR models and to calculate a pharmacophore model. Our goal, more importantly, is to apply the pharmacophore model to search structurally diverse molecular databases to prospectively identify novel nAChR inhibitors. The successful identification of novel molecules using computational models and the demonstration of their in vitro activity are valuable tools for the efficient retrieval of novel or hitherto unrecognized nAChR inhibitors, potentially leading to subtype-selective nAChR antagonists.

Materials and Methods

Materials. (−)Nicotine hydrogen tartrate, polyethyleneimine, and components of N2+ media were obtained from the Sigma Chemical Co. (St. Louis, MO). Dulbecco's modified Eagle's medium, Dulbecco's modified Eagle's medium/F-12 (used in N2+ medium), minimum essential medium, antibiotics, and L-glutamine were obtained from Invitrogen Corporation (Carlsbad, CA). Fluo-4-acetoxymethylester, probenecid, and Pluronic F-127 were obtained from Molecular Probes (Eugene, OR). (±)[5,6-bicycloheptyl-^{3}H]Epibatidine (specific activity, 55.5 Ci/mmol) and DL-[7-^{3}H(*N*)]norepinephrine hydrochloride (specific activity, 10–15 Ci/mmol) were purchased from PerkinElmer Life and Analytical Sciences (Boston, MA). Whatman GF/B filters were purchased from Brandel Laboratories, Inc. (Gaithersburg, MD). Bovine adrenal glands were purchased from the Herman Falter Packing Company (Columbus, OH). MLA analogs (Figs. 1 and 9) were in general prepared by reaction of hydroxymethyl piperidine with the appropriate alkyl halide to provide the *N*-alkyl hydroxymethyl piperidine. This compound was then coupled to the appropriate carboxylic acid to provide the target MLA analog (Bergmeier et al., 2004). All compounds were pure as shown by ^{1}H NMR, ^{13}C NMR, and high-resolution mass spectrometry.

Neurosecretion Studies. Bovine adrenal chromaffin cells were dissociated from intact glands and placed into culture as described previously by our laboratory (Maurer and McKay, 1994). A [^{3}H]norepinephrine assay was used to monitor neurosecretion from cultured cells (Maurer and McKay, 1994). Cells were typically used experimentally 4 to 7 days after isolation. Cells were pretreated for 15 min with the analogs before stimulation with nicotine (10 μM) in the continued presence of the analog. Because of solubility problems, IC_{50} values of a few analogs (APBs 1, 4, and 11) could not be precisely determined; values of 10 μM for these analogs were used for modeling purposes. Results were calculated from the number of observations (n) performed in duplicate or triplicate. IC_{50} values were obtained by averaging values generated from nonlinear regression analyses (Prism; GraphPad Software Inc., San Diego, CA) of individual concentration-response curves. Concentration-response data are expressed as geometric means (95% confidence limits). Linear regression analyses were performed using Prism with the level of significance set at $p < 0.05$.

[^{3}H]Epibatidine Binding to Native and Recombinant $\alpha3\beta4$ nAChRs. Membrane preparations from bovine adrenal medullary tissues were prepared, and agonist binding experiments were performed as described previously by our laboratory (Free et al., 2002). In brief, adrenal membranes were incubated at room temperature for 60 min in 500 μl of assay/rinse buffer (120 mM NaCl, 5 mM KCl, 8 mM Na_2HPO_4, 0.1 mM phenylmethylsulfonyl fluoride, 5 mM iodoacetamide, 2 mM EDTA, 2 mM EGTA, and 5 mM HEPES, pH 7.4) containing 1 nM [^{3}H]epibatidine. α-Bungarotoxin (1 μM) was added to the buffer to eliminate potential radiolabeled ligand binding to α-bungarotoxin binding sites. For the analog competition binding studies, membranes were incubated without (control) or with 10 μM concentrations of the analogs. Nonspecific binding was determined in the presence of 300 μM nicotine (typically 5–10% of total binding). A HEK 293 cell line stably expressing bovine $\alpha3\beta4$ nAChRs (BM$\alpha3\beta4$ cells) developed by our laboratory was used as a rich source of recombinant bovine adrenal $\alpha3\beta4$ nAChRs (Free et al., 2002). nAChR binding experiments using BM$\alpha3\beta4$ cell membrane preparations were performed by modification of procedures described previously by our laboratory (Free et al., 2003). In brief, HEK cell membranes were prepared using mammalian protein extraction reagent according to the manufacturer's instructions and with the addition of a protease inhibitor cocktail (Roche, Indianapolis, IN). Membranes were incubated at room temperature for 60 min in a binding/rinse buffer containing 1 nM [^{3}H]epibatidine. For the analog competition binding studies, membranes were incubated without (control) or with 10 μM concentrations of the analogs. Nonspecific binding was determined in the presence of 300 μM nicotine. Specific binding was determined by subtracting nonspecific binding (typically 1–2% of total binding) from total binding.

Measurement of Intracellular Calcium Using HEK 293 Cells Stably Expressing Recombinant nAChRs. For theses studies, BM$\alpha3\beta4$ cells that express bovine adrenal $\alpha3\beta4$ nAChRs and KX$\alpha3\beta4$R cells (Xiao et al., 1998) that express rat $\alpha3\beta4$ nAChRs were used. Cells were plated on poly(D-lysine)-coated 96-well plates at a density of 1.2 to 1.5 × 10^5 cells/well and incubated at 37°C in 5% CO_2 using minimum essential medium supplemented with 10% fetal bovine serum, 10 mM L-glutamine, 0.7 mg/ml G-418, 100 U/ml penicillin, and 100 μg/ml streptomycin. Forty-eight hours after plating, cells were washed with HEPES-buffered Krebs solution (155 mM NaCl, 4.6 mM KCl, 1.2 mM $MgSO_4$, 1.8 mM $CaCl_2$, 6 mM glucose, and 20 mM HEPES, pH 7.4) for KX$\alpha3\beta4$R cells or with HEPES-buffered Krebs solution with 20 mM $CaCl_2$ for BM$\alpha3\beta4$ cells and loaded with 2 μM Fluo-4-acetoxymethylester in the presence of 2.5 mM probenecid and 0.05% Pluronic F-127 for 1 h at 24°C and

protected from light. At the end of the incubation period, the cells were washed once more, and basal fluorescence was measured using a fluid-handling integrated fluorescence plate reader (Flex Station; Molecular Devices, Sunnyvale, CA). Responses after addition of agonists were recorded for 20 s. When analogs were tested, cells were preincubated for 40 s before stimulation in the continued presence of the analog. Probenecid (2.5 mM) was included in all of the solutions once the cells were loaded to prevent the leakage of Fluo-4 from the cell. The Fluo-4 fluorescence was read at an excitation of 494 nm and an emission of 520 nm from the bottom of the plate.

Molecular Modeling and Structure Building. The computational molecular modeling studies were carried out using an Octane workstation (SGI, Mountain View, CA) with the IRIX 6.5 operating system running the SYBYL software suite version 6.9 (Tripos Inc., St. Louis, MO). The molecular structures of the analogs were built using standard bond distances and bond angles with the sketch module of SYBYL. All molecules were charged according to physiological conditions. Partial atomic charges were then calculated using the Gasteiger-Marsili method. The energy minimizations were performed using Tripos force field with a distance-dependent dielectric coefficient and the Powell conjugate gradient algorithm with an energy change convergence criterion of 0.001 kcal/mol.

Genetic Algorithm Similarity Program. Genetic Algorithm Similarity Program (GASP) is a genetic algorithm developed for the perception of pharmacophore models through superimposition of flexible molecules (Jones et al., 1995). When aligning a set of molecules, GASP attempts to optimize the orientation and conformation of molecules at the same time by quickly and efficiently fitting them to similarity constraints. One major limitation of GASP is that each run can only align four to five molecules depending on the molecular complexity. To align all 67 compounds using GASP, they were separated into 19 groups of either 4 or 5 compounds, each containing the model compound IB 12. Compounds in each group were aligned to IB 12 using GASP. All aligned structures from different groups were subsequently merged together and used as input for later CoMFA and CoMSIA studies. When generating the alignment, to broaden the diversity of conformations that were considered, the "population size" was increased to 125 and the "allele mutate weight" to 96. With increased population size and mutation rates, conformations with more diversity were generated. To avoid possible problems with convergence because of the increased mutation rate, the convergence criteria were loosened by increasing the "fitness increment" to 0.02. Ten alignments were generated, and the best model was selected through visual inspection based on chemical intuition.

To generate a pharmacophore model for this set of analogs, four representative potent analogs (IB 12, IB 9, PPB 3, and PPB 13) were selected. The most potent, IB 12, was chosen as the template for alignment. The same GASP settings were maintained for pharmacophore generation.

CoMFA. SYBYL/CoMFA is a successful implementation of 3D-QSAR technique that explains the gradual changes in observed biological properties by evaluating the electrostatic (Coulombic interactions) and steric (van der Waals interactions) fields at regularly spaced grid points surrounding a set of mutually aligned ligands (Cramer et al., 1988). The interaction fields were calculated using an sp^3 hybridized carbon probe atom (+1 charge at 1.52 Å van der Waals radius) on a 2.0 Å spaced lattice, which extends beyond the dimensions of each structure by 4.0 Å in all directions. Because of the steep steric and electrostatic potential functions when the probe atom is placed close to the molecule van der Waals surface, a cutoff value of 30 kcal/mol was set to ensure that no extreme energy terms will distort the final model. To reduce chance correlation and effectively correlate the huge number of field descriptors with relatively few biological activities, the statistical algorithm partial least square was adopted (Clark and Cramer, 1993). The indicator fields (Kroemer and Hecht, 1995) and hydrogen bond fields (Bohacek and McMartin, 1992) generated by the "advanced CoMFA" module were also included in the analysis. Among the 67 tested analogs, 6 were randomly selected as the test set, and the rest (61) were used as a training set for model generation. CoMFA descriptors were used as independent variables, whereas the dependent variable (biological descriptor) used in these studies was the negative logarithm of the analog IC_{50} values ($-\log IC_{50}$) for their inhibition of $\alpha3\beta4$ nAChR-mediated bovine adrenal neurosecretion. The predictive value of the models was initially evaluated using leave-one-out cross-validation. The cross-validated coefficient, q^2, is calculated as follows:

$$q^2 = 1 - \frac{\sum_Y (Y_{predicted} - Y_{observed})^2}{\sum_Y (Y_{observed} - Y_{mean})^2}$$

where $Y_{predicted}$, $Y_{observed}$, and Y_{mean} are the predicted, observed, and mean values of the target property ($-\log IC_{50}$), respectively. $\Sigma(Y_{predicted} - Y_{observed})^2$ is the predictive error sum of squares (PRESS). The standard error of the cross-validated predictions is known as "press," and the root mean square of the conventional (non–cross-validated) predictions is labeled "s." The model with the optimum number of principal components, corresponding to the lowest PRESS value, was selected for deriving the final partial least square regression models (Table 1). Contour of standard coefficients enclosing the most significant value was plotted (Fig. 3).

CoMSIA. SYBYL/CoMSIA is an extension of CoMFA methodology developed by Klebe and colleagues (1994). They differ only in the implementation of the interaction fields. Instead of using Lennard-Jones potential (steric fields) and Coulombic potential (electrostatic fields), CoMSIA uses a Gaussian-type function to avoid the extreme values generated by the two functions, thus eliminating the requirement of setting a cutoff value in field generation process. The Gaussian function also results in smoother, less fragmented surfaces in the final model representation. Five physicochemical properties (steric, electrostatic, hydrophobic, hydrogen bond donor, and hydrogen bond acceptor) were evaluated using a positively charged sp^3 hybridized carbon probe atom. The same set of training set and test set compounds with identical alignment from the CoMFA study was used for the generation and evaluation of the CoMSIA model. A field contour was similarly plotted (Fig. 4).

UNITY. UNITY (Tripos Inc.) is a database screening and analyzing tool that is capable of 2D and 3D searches. It performs flexible 3D database searching by implementing the directed tweak technique (Hurst, 1994). A UNITY query was prepared by extracting the chemical features and the feature constraints from the previously generated GASP pharmacophore model. The query was subsequently modified to optimize both specificity and selectivity. Flexible searches of 445,742 compounds from both Chembridge (241,903 compounds) and Spec (203,839 compounds) databases were performed. The distance constraints tolerance was increased from the default 0.1 to 0.5 Å to increase the chance of retrieving more diversified hit compounds.

Results

Our laboratory has synthesized a library of analogs of MLA. Although MLA itself is a competitive inhibitor of both native (Free et al., 2002) and recombinant (Free et al., 2003) $\alpha3\beta4$ nAChRs, our data support the inhibitory activity of

TABLE 1
Statistics for CoMFA and CoMSIA models

	q^2	PRESS	n	r^2	S	Steric	Electrostatic	q^{2a}
						%	%	
CoMFA	0.648	0.301	3	0.853	0.194	53	47	0.904
CoMSIA	0.767	0.247	4	0.906	0.16	75[b]	25[c]	0.946

[a] Test set prediction.
[b] Percentage of hydrophobic interaction.
[c] Percentage of H-bond acceptor interaction.

several MLA analogs as noncompetitive in nature (Bergmeier et al., 1999, 2004; Bryant et al., 2002). In the following studies, the concentration-response effects of 67 analogs of MLA on nicotine-stimulated adrenal neurosecretion were investigated (Fig. 1), and their IC_{50} values are listed in Table 2. The IC_{50} values of the analogs ranged from 0.9 to 115 μM with a median IC_{50} value of 3.7 μM. In the concentration ranges tested ($\leq$10 μM), these analogs have little or no inhibitory effects on agonist binding to recombinant and native nAChRs, with mean binding effects that are 118.4 $\pm$ 2.7% of control, ranging from 69% of control to 174% of control. Only ~4% (3/67) of the analogs at concentrations of 10 μM produced decreases of $\geq$15% in nAChR binding and ~48% (32/67) of the analogs produced apparent increases ($\geq$115% of control) in $\alpha3\beta4$ nAChR binding assays at concentrations of 10 μM. For several of the analogs, their direct effects on nAChRs were assessed using cell lines expressing recombinant nAChRs. As noted in Tables 3 and 4, the analogs inhibit nicotine-induced increases in free intracellular calcium level with little or no inhibitory effects on agonist binding to nAChRs. These data are consistent with our previous data supporting noncompetitive nAChR inhibition.

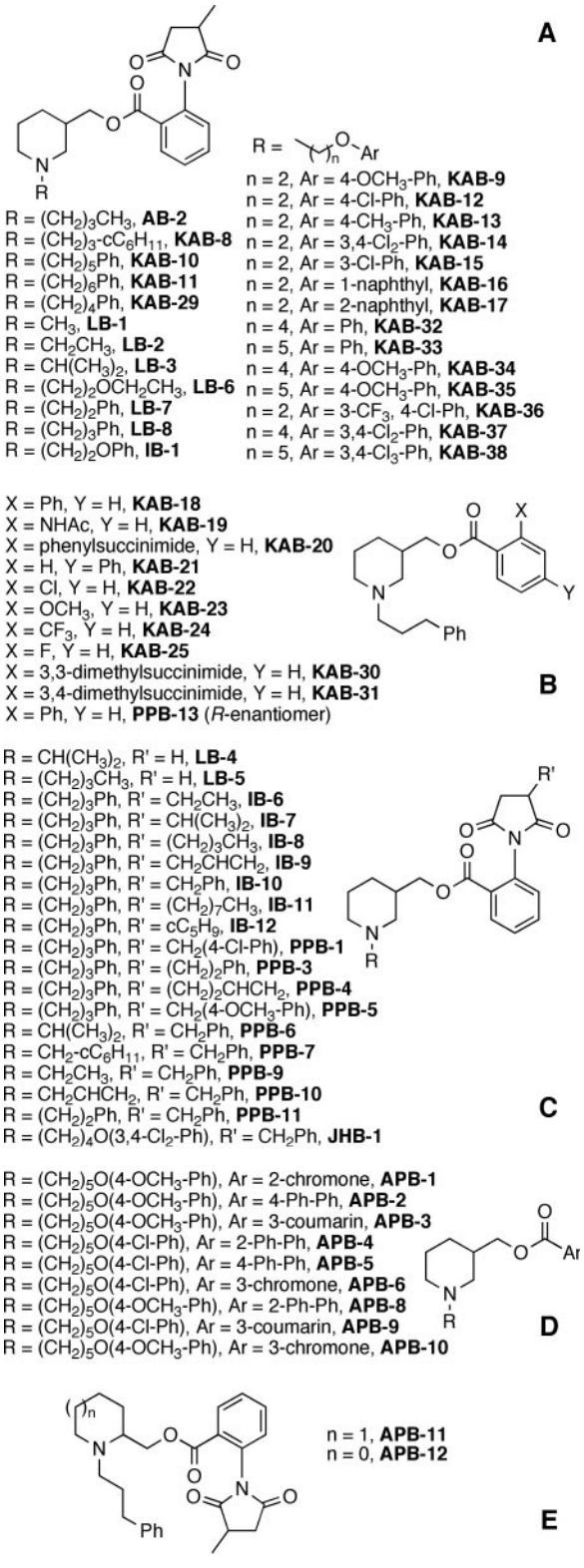

Fig. 1. Structures of compounds listed in Tables 2 and 3.

All 67 MLA analogs were favorably aligned using GASP-guided subgroup alignment (Fig. 2). Subsequent 3D-QSAR analyses were successfully carried out based on this alignment. The statistical significance of the CoMFA model is indicated by a cross-validated r^2 (q^2) value of 0.648 (Table 1). The model has a correlation of 0.853 (r^2), with electrostatic and steric interactions contributing similarly. The model's predictive power is further corroborated by the predictive r^2 value of 0.904 when applied to an independent test set (Table 1). The alignment of CoMFA fields with the substrate, IB 9, is shown in Fig. 3. The IB 9 backbone is covered by yellow contours, which essentially delineates the shape of the receptor-binding cavity because these regions represent areas of steric hindrance. The green contour (α) over the phenyl group emphasizes the importance of a sterically bulky group in this binding pocket, probably providing favorable hydrophobic interactions. Likewise, the green contour (β) illustrates the importance of a succinimide group to fill in another binding pocket. The large blue contour (γ) over the ammonium group emphasizes the essential role of a positive charge at this position. The red contour (δ) over the ester carbonyl group and the oxygen atom indicates that negative charges at these positions are favorable for optimum binding.

Based on the same alignment, the CoMSIA model also shows good correlation (r^2 = 0.906) between hydrophobic, hydrogen-bond acceptor (HBA) interactions and inhibition of neurosecretion. The highly predictive nature of the model is supported by the leave-one-out cross-validation and external test set prediction (q^2 of 0.767 and r^2 of 0.946, respectively; Table 1). When the CoMSIA coefficients are plotted with substrate IB 9 (Fig. 4), the large areas surrounding the backbone of IB 9 are covered by yellow contours, which delineate shape requirements of the binding pocket and correlate with unfavorable hydrophobic interactions. The two green contours indicate the important hydrophobic interactions with the phenyl ring (α) and the succinimide group (β). The blue contour (γ) suggests favorable interactions between amide carbonyl groups (as HBAs) and the binding pocket. The large red contour (δ) suggests the overall preference of less HBA for analog binding.

Table 3 shows the predicted CoMFA and the predicted CoMSIA IC_{50} values and the experimentally derived functional IC_{50} values for the six test set compounds (IB 10, KAB 13, KAB 34, LB 6, PPB 5, and PPB 11). Linear regression analyses of these data (Fig. 5) reveal significant correlation ($p < 0.05$) between predicted CoMFA and CoMSIA IC_{50} val-

TABLE 2
Effects of analogs on adrenal neurosecretion
Concentration-response effects of the analogs were determined as described under *Materials and Methods*; IC_{50} values represent geometric means (confidence limits), $n = 3$ to 7.

Figure 1A		Figure 1B		Figure 1C		Figure 1D		Figure 1E	
Analog	Nicotine-Stimulated Neurosecretion (IC_{50})	Analog	Nicotine-Stimulated Neurosecretion (IC_{50})	Analog	Nicotine-Stimulated Neurosecretion (IC_{50})	Analog	Nicotine-Stimulated Neurosecretion (IC_{50})	Analog	Nicotine-Stimulated Neurosecretion (IC_{50})
	μM		μM		μM		μM		μM
KAB 37	1.9 (1.6–2.2)	PPB 13	0.9 (0.8–1.1)	PPB 3	1.0 (0.9–1.2)	APB 3	2.1 (1.5–2.8)	APB12	13.0 (11–16)
KAB 36	2.0 (1.8–2.2)	KAB 20	1.3 (1.2–1.6)[a]	PPB 5[b]	1.2 (1.1–1.3)	APB 2	2.8 (2.5–3.1)	APB11	≥ 10
KAB 14	2.1 (1.9–2.4)	KAB 18	1.7 (1.6–1.8)[a]	PPB 7	1.2 (1.1–1.3)	APB 8	2.8 (2.1–3.9)		
KAB 16	2.5 (2.3–2.8)	KAB 21	3.0 (2.3–3.9)[a]	IB 12	1.2 (1.2–1.3)	APB 9	4.0 (3.2–4.8)		
KAB 17	2.7 (2.3–3.1)	KAB 23	3.2 (3.1–3.4)[a]	IB 10[b]	1.3 (1.1–1.4)[a]	APB 6	6.6 (6.1–7.2)		
KAB 11	2.8 (2.4–3.1)	KAB 24	3.2 (3.1–3.2)[a]	IB 11	1.3 (0.7–2.4)[a]	APB 5	7.1 (5.8–8.7)		
KAB 35	3.3 (2.8–3.9)	KAB 22	3.4 (3.2–3.5)[a]	JHB 1	1.3 (1.1–1.5)	APB10	8.2 (6.2–9.8)		
KAB 10	3.5 (3.5–3.6)	KAB 25	5.2 (4.8–5.6)[a]	PPB 4	1.3 (1.2–1.3)	APB 4	≥ 10		
KAB 38	3.5 (3.2–3.8)	KAB 31	6.0 (5.5–6.6)[a]	IB 8	1.5 (1.5–1.5)[a]	APB 1	≥ 10		
KAB 12	3.7 (3.4–3.9)	KAB 30	7.5 (6.8–7.6)[a]	PPB 6	1.6 (1.6–1.7)				
KAB 33	4.2 (3.6–4.9)	KAB 19	8.4 (7.8–9.1)[a]	PPB 1	1.7 (1.5–1.9)				
KAB 13[b]	4.4 (4.3–4.6)			IB 9	1.7 (1.7–1.7)[a]				
KAB 15	4.6 (4.0–5.3)			IB 7	2.5 (2.3–2.6)[a]				
KAB 29	5.3 (5.0–5.5)			PPB 11[b]	2.6 (2.2–3.1)				
KAB 8	5.4 (5.0–5.8)			IB 6	4.0 (3.7–4.3)[a]				
KAB 34[b]	6.2 (5.3–7.2)			PPB 10	4.1 (3.8–4.5)				
KAB 32	6.7 (6.0–7.5)			PPB 9	5.7 (5.0–6.5)				
KAB 9	6.9 (6.5–7.3)			LB 5	65 (53–80)[c]				
LB 8	11 (10–12)[c]			LB 4	114 (96–138)[c]				
IB 1	20 (19–21)[c]								
AB 2	27 (24–32)								
LB 3	37 (28–48)[c]								
LB 7	52 (48–57)[c]								
LB 6[b]	59 (55–63)[c]								
LB 1	63 (55–73)[c]								
LB 2	62 (59–66)[c]								

[a] Data are from Bergmeier et al. (2004).
[b] Test set compound.
[c] Data are from Bryant et al. (2002).

ues and experimentally derived functional IC_{50} values (r^2 values of 0.90 and 0.81, respectively). In addition, the effects of the test set analogs on agonist binding to native and recombinant bovine nAChRs and their effects on the functional activation of native and recombinant nAChRs are compared. The analogs inhibit activation of recombinant nAChRs and inhibit adrenal neurosecretion at similar concentrations and have little or no inhibitory effects on agonist binding to either native or recombinant nAChRs.

The GASP-generated pharmacophore model, based on four structures, contains 10 feature points with an average interpoint distance of 5.43 Å. This machine-generated pharmacophore model was further improved based on knowledge of all 67 compounds and chemical intuition. More specifically, feature points that are specific to a certain structure series and duplicate feature points indicating identical pharmacophore features were removed. The resulting more general UNITY query contains three hydrophobes, two HBAs, and one positively charged nitrogen atom (Fig. 6). This knowledge-based pharmacophore model was used to flexibly search two commercially available databases. The resulting hit lists simultaneously served as a means of model validation and assisted in the selection of molecules for subsequent in vitro testing. The data mining yielded multiple hits, eight of which were commercially available compounds. Structures of these compounds are found in Fig. 7, and their predicted IC_{50} values are listed in Table 5. None of these compounds inhibited agonist interactions using $\alpha3\beta4$* nAChR binding assays (data not shown). The concentration-response effects of the compounds on adrenal neurosecretion were investigated. Indeed, all proposed compounds inhibited adrenal neurosecretion (Table 5) even though no significant correlations are found when predicted IC_{50} values are plotted versus experimentally derived IC_{50} values (Fig. 8A). This result suggests that when applied to chemical spaces outside those of the training set, our computational model predictions should be interpreted qualitatively (identifying noncompetitive nAChR inhibitors) rather than quantitatively (predicting exact IC_{50} values of these inhibitors).

To further validate the QSAR model, several new MLA analogs were synthesized (Fig. 9). COB 1, COB 2, COB 3, and DDR 1 are potent inhibitors of adrenal neurosecretion and inhibit functional activation of recombinant nAChRs (Table 4). Once again, no inhibition of agonist binding to $\alpha3\beta4$* nAChRs was observed with these compounds. QSAR predictions of their IC_{50} values are comparable with their experimentally derived functional IC_{50} values (Table 4). Linear regression analyses of these data reveal no significant correlations (Fig. 8B). Once again, these data support the qualitative, rather than the quantitative, nature of the model.

Discussion

The principal receptors mediating adrenal neurosecretion are $\alpha3\beta4$* nAChRs (Gu et al., 1996; Free et al., 2002, 2003), with the asterisk indicating the possible presence of additional subunits (Lukas et al., 1999; Free et al., 2003). Our laboratory (Bergmeier et al., 1999, 2004; Bryant et al., 2002) and others (Barker et al., 2005) have reported previously the synthesis of several analogs of MLA that seem to act as noncompetitive inhibitors of $\alpha3\beta4$* nAChRs. Noncompetitive inhibitors are defined as those compounds that do not com-

TABLE 3

Comparison of predicted and experimentally derived IC_{50} values of test set compounds

Competition binding experiments were performed at a fixed concentration of each analog (10 μM), as described under *Materials and Methods*; values represent arithmetic means ± S.E.M., n = 3 to 7. Native nAChR nicotine-stimulated neurosecretion data are from Table 2. Inhibition curves were generated as described under *Materials and Methods*; values represent geometric means (confidence limits), n = 4.

Analog	IC_{50} Values				nAChR Specific Binding	
	CoMFA	CoMSIA	Native nAChR Nicotine-Stimulated Neurosecretion	Recombinant nAChR Nicotine-Stimulated $[Ca^{2+}]_i$	Native nAChRs	Recombinant nAChRs
			μM		*% Control*	
IB 10	1.2	1.3	1.3 (1.1–1.4)	7.6 (6.8–8.6)	151.3 ± 15.7	99.6 ± 0.4
KAB 13	7.2	4.0	4.4 (4.3–4.6)	N.D.	114.3 ± 1.4	95.0 ± 0.9
KAB 34	2.8	3.0	6.2 (5.3–7.2)	3.1 (2.8–3.5)	83.2 ± 1.4	88.2 ± 11.6
LB 6	40.7	47.9	59.6 (55.6–63.9)	N.D.	92.4 ± 4.9[a]	N.D.
PPB 5	1.5	1.6	1.2 (1.1–1.3)	13.4 (10.3–17.3)	152.8 ± 7.6	90.8 ± 1.6
PPB 11	1.4	1.9	2.6 (2.2–3.1)	8.0 (5.9–10.8)	118.4 ± 12.5	99.9 ± 12.3

N.D., not determined.
[a] Competition binding experiments were performed at a fixed antagonist concentration of 100 μM.

TABLE 4

Comparison of predicted and experimentally derived IC_{50} values of MLA analogs

Predicted IC_{50} values were calculated using the CoMFA model. Inhibition curves were generated as described under *Materials and Methods*; values represent geometric means (confidence limits), n = 4 to 6. Competition binding experiments were performed with a fixed concentration of each analog (10 μM), as described under *Materials and Methods*; values represent arithmetic means ± S.E.M., n = 4.

Analog	IC_{50} Values			Native nAChR Specific Binding
	CoMFA Prediction	Native nAChR Nicotine-Stimulated Neurosecretion	Recombinant nAChR Nicotine-Stimulated $[Ca^{2+}]_i$	
		μM		*% Control*
COB 1	2.7	3.5 (3.1–3.9)	1.2 (1.0–1.4)	113.5 ± 4.8
COB 2	9.8	1.2 (1.2–1.3)	1.1 (1.0–1.1)	125.8 ± 3.8
COB 3	6.1	3.0 (2.5–3.7)	0.7 (0.6–0.9)	106.0 ± 2.5
DDR 1	11.5	1.7 (1.4–2.0)	30.0 (23.5–38.3)	118.7 ± 13.9

pete for binding at the agonist binding site and yet still bind to the receptor and produce functional effects. In this study, two approaches were used to characterize functional effects of our molecules. Both nicotine-stimulated neurosecretion assays on adrenal chromaffin cells and nicotine-stimulated intracellular calcium measurements using a cell line expressing bovine $\alpha 3\beta 4$ nAChRs were used to identify functional effects of the analogs mediated via native and recombinant nAChRs, respectively. In the second approach, the nicotine-stimulated increase in intracellular calcium is through nAChR-associated ion channels; therefore, inhibition of nicotine-stimulated increases in intracellular free calcium supports a direct action of the analogs on nAChRs. Agonist binding experiments confirm that the analogs are not competitive antagonists. As shown in Table 3, the test set analogs inhibited nicotine-induced increases in intracellular free calcium but had little or no inhibitory effects on agonist binding to recombinant nAChRs. Similar data have been obtained with an additional 30 analogs (data not shown). These data support noncompetitive interactions of the analogs on $\alpha 3\beta 4$ nAChRs.

Although most investigations into nAChR drug development have used recombinant nAChRs, these studies have

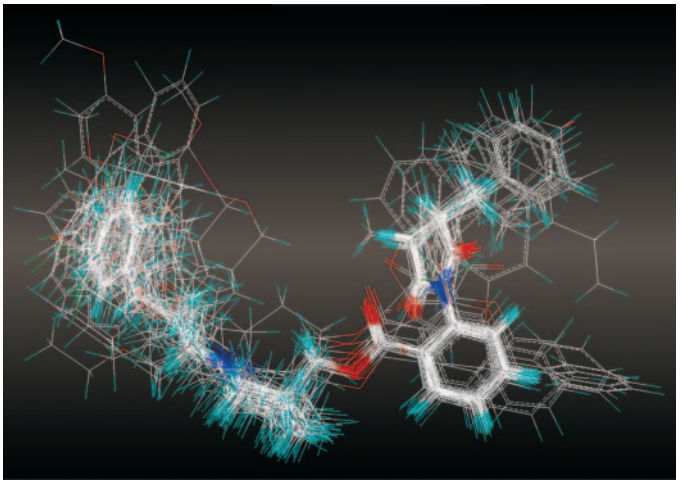

Fig. 2. Overall alignment of all 67 compounds used in generating the following 3D-QSAR models. All 67 structures are shown as wireframe representation.

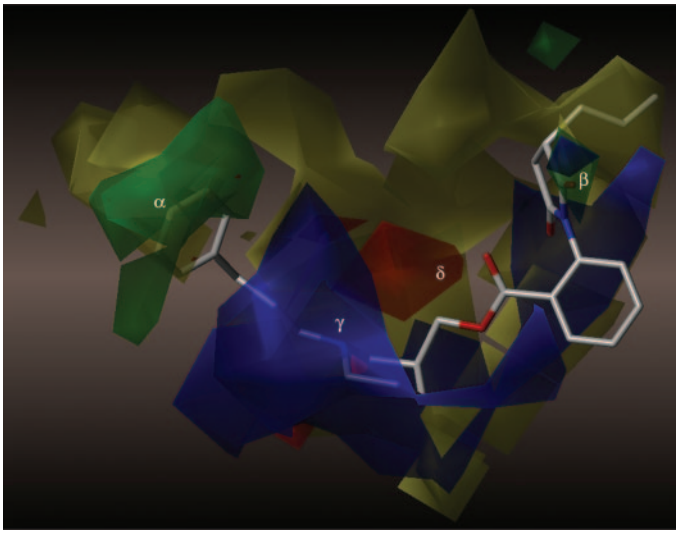

Fig. 3. CoMFA model of analog binding. CoMFA coefficient contours map aligned with inhibitor IB 9. The contours of the steric map are shown in yellow and green, whereas the contours of the electrostatic map are shown in red and blue. Greater antagonism (lower IC_{50} values) is correlated with less bulk near yellow (17%), more bulk near green (20%), more negative charge near red (20%), and more positive charge near blue (20%).

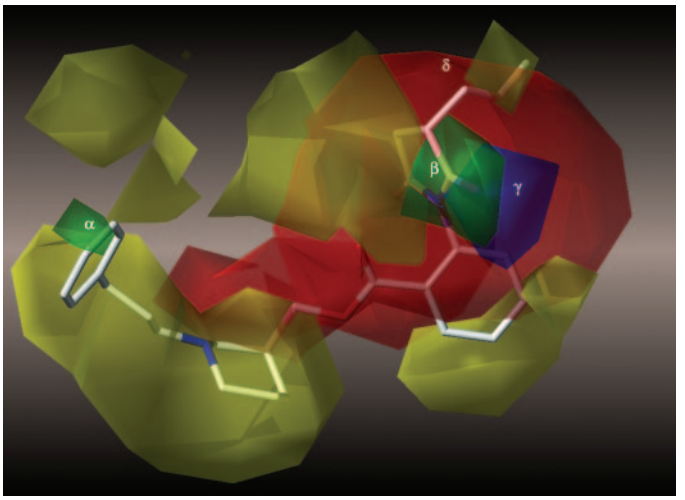

Fig. 4. CoMSIA model of pharmacophore. CoMSIA contours aligned with inhibitor IB 9. The contours of the hydrophobic map are shown in yellow and green, whereas the contours of the HBA map are shown in red and blue. Greater inhibition (lower IC_{50} values) is correlated with less bulk near yellow (18%), more bulk near green (20%), more HBA near blue (20%), and less HBA near red (20%).

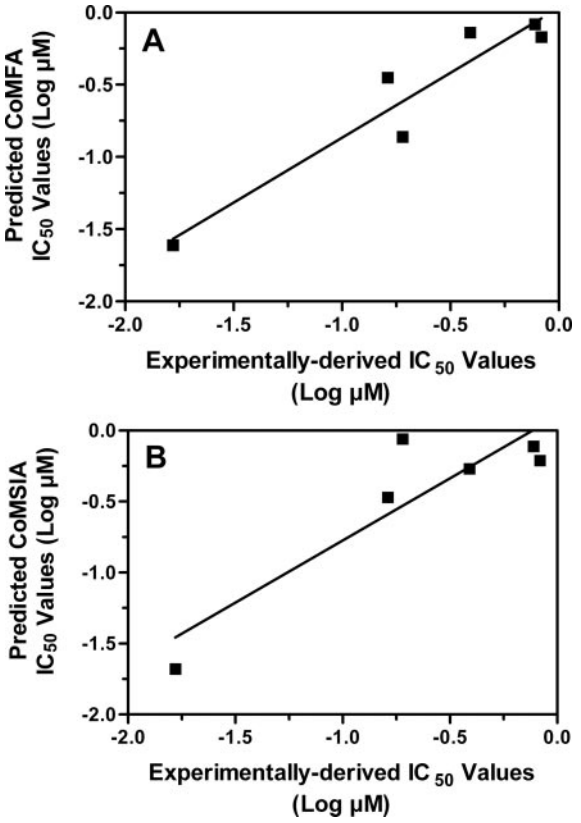

Fig. 5. Linear regression analyses of predicted and experimentally derived functional IC_{50} values of test set compounds. Predicted and experimentally derived functional IC_{50} values of test set compound (IB 10, KAB 13, KAB 34, LB 6, PPB 5, and PPB11) using CoMFA model (A) or CoMSIA model (B). IC_{50} values of test set compounds are listed in Table 2.

focused on native nAChRs. Whereas there are inherent disadvantages of this approach, one being that the exact subunit composition of the native nAChRs is not known, this approach is likely to yield a better understanding of physiological attributes of the analogs and potential pitfalls in drug design that are not apparent from conventional assays using cells expressing recombinant receptors. These assays involving recombinant nAChRs do not take into account potential analog interactions with other proteins (e.g., additional receptors, ion channels) found in the native environment, leaving out any effects generated by them. Another problem involves the site of action of the analogs or the data-mined molecules. It cannot be established from these studies where these compounds are binding on the receptor protein and whether they bind to a single site or multiple sites on $\alpha 3\beta 4^*$ nAChRs. It is well established that multiple noncompetitive binding sites exist on nAChRs (Lloyd and Williams, 2000). One of these sites is located within the nAChR ion channel. This site has been fairly well characterized in muscle nAChRs (Le Novere and Changeux, 1995). Other "sites" have been described simply as locations at the lipid-protein interface. These studies also do not address whether these analogs show nAChR subtype-selectivity or whether the computational models/pharmacophore applies to other nAChR subtypes. Studies involving the localization of the noncompetitive binding site on nAChRs and subtype-specificity of the analogs are currently in progress.

In these studies, the pharmacological activities of 67 MLA

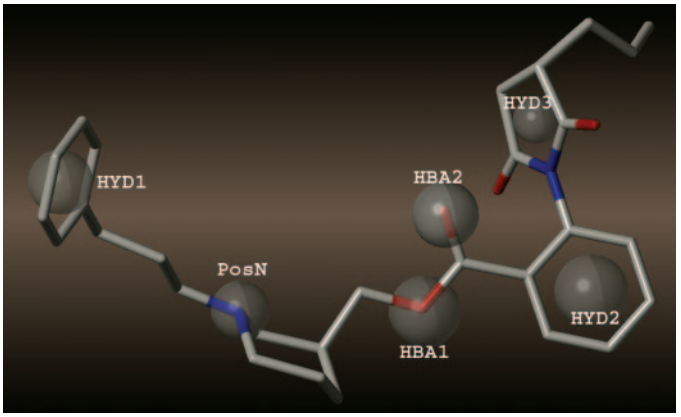

Fig. 6. Pharmacophore model generated using GASP. The pharmacophore features are illustrated using IB 9. HYD, hydrophobic feature; HBA, hydrogen bond acceptor feature; PosN, positively charged nitrogen feature.

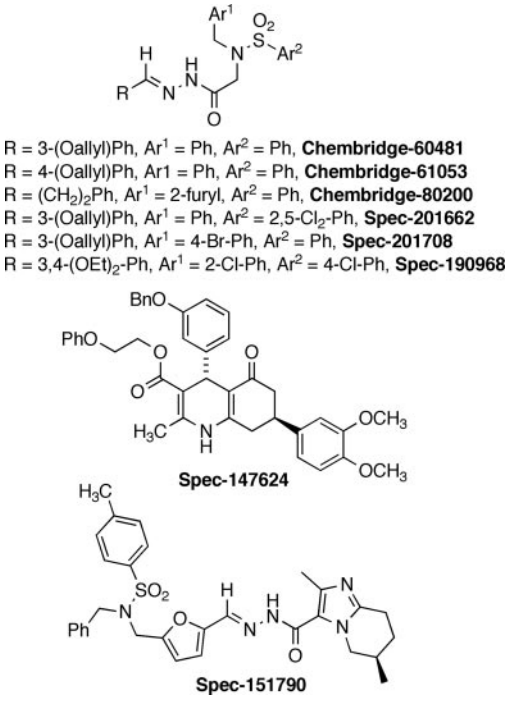

Fig. 7. Structures of compounds listed in Table 5.

TABLE 5

Comparison of predicted and experimentally derived IC_{50} values from hit compounds returned from database screening

Predicted IC_{50} values were calculated using CoMFA model. Functional inhibition curves were generated as described under *Materials and Methods*; values represent geometric means (confidence limits), $n = 3$ to 5.

Compound	IC_{50} Values	
	Predicted	Experimentally Derived
		μM
Chembridge 60481	5.0	9.7 (6.9–12)
Chembridge 61053	17.2	7.7 (6.7–8.8)
Chembridge 80200	14.7	6.1 (4.9–7.6)
Spec 151790	29.5	7.4 (6.5–8.5)
Spec 147624	7.9	49.5 (24.7–99.5)
Spec 201662	11.8	15 (11.9–19.0)
Spec 201708	9.9	12.4 (11.5–13.4)
Spec 190968	25.6	33.9 (31.6–36.3)

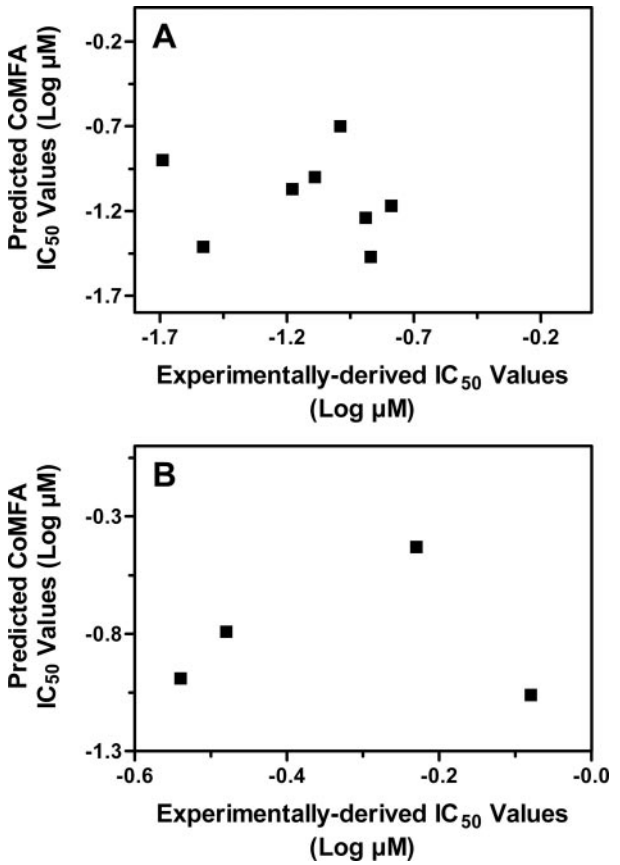

Fig. 8. Comparison of predicted and experimentally derived functional IC_{50} values. A, predicted and experimentally derived functional IC_{50} values of compounds obtained from data mining (A) and new MLA analogs not used in pharmacophore modeling (B). Predicted and experimentally derived IC_{50} values are found in Tables 4 (B) and 5 (A).

analogs were investigated, and a putative noncompetitive nAChR recognition site and a noncompetitive pharmacophore are proposed. Few studies have had such a wealth of structurally similar compounds for analyses. We have found that the more potent of these MLA analogs have functional IC_{50} values in the low micromolar range, similar to potencies of other antagonists of adrenal neurosecretion including hexamethonium, decamethonium, *d*-tubocurarine, tetracaine, pentolinium, and mecamylamine (IC_{50} values ranging for 17 to 0.1 μM) (McKay and Sanchez, 1990; McKay and Burkman, 1993). In addition, two classic noncompetitive inhibitors of muscle nAChRs, phencyclidine and histrionicotoxin, have affinities in the micromolar and submicromolar range (~1 and ~0.3 μM, respectively) (Heidmann et al., 1983). Through structural modification of our compounds, we have increased potencies of these compounds into ranges that currently exist for noncompetitive nAChR antagonists, supporting the use of MLA analogs to elucidate structural determinants important for nAChR activity.

The conventional target for drug development has been the agonist binding site of nAChRs, located on α nAChR subunits. Not unexpectedly, the binding sites on different α subunits have a high degree of amino acid similarity. From an evolutionary perspective, selective pressure has forced this similarity as a result of interaction of these sites with the endogenous neurotransmitter acetylcholine. The lack of pharmacologically specific agonists and antagonists directed at these sites is probably related to the physiochemical resemblance of agonist binding sites. The selectivity of most agonists and competitive antagonists is modest at best. As a novel approach for neuronal nAChR drug discovery, our laboratory has targeted other sites (noncompetitive sites, negative allosteric binding sites) located on nAChRs. Similar approaches were used on $GABA_A$ receptors (Olsen et al., 2004), and the discovery of the benzodiazepine binding site has led to an important therapeutic class of drugs.

Pharmacophore development for noncompetitive nAChR binding sites is hampered by a lack of specific, high-affinity, radiolabeled ligands. The availability of native cells expressing neuronal nicotinic receptors, functional assays for studies on the pharmacological effects of molecules, and a large number of structurally related molecules presented a unique opportunity for the development of a pharmacophore model for noncompetitive binding sites. Indeed, two 3D-QSAR models and one pharmacophore model were successfully generated based on these data. The CoMFA model explained the binding affinity using steric and electrostatic interactions, whereas the CoMSIA model correlated the same activity with hydrophobic and HBA interactions. Both the CoMFA and CoMSIA models clearly delineated the binding pocket. In addition, the CoMFA model identified the positive charge provided by the amine group and the negative charge carried by the ester carbonyl group as essential for binding. The CoMSIA model emphasized the important role of the amide carbonyl group from the succinimide ring as an HBA needed in docking to the binding site. Both models were highly predictive in calculating an external test set. They also successfully categorized the retrieved compounds from pharmacophore-based database screening.

With three hydrophobic features, two HBAs, and one positively charged nitrogen atom, the pharmacophore prototype echoes the findings of 3D-QSAR models and provides more direct visualization of binding requirements (Fig. 6). The prospective application of this pharmacophore model in screening two commercial molecule databases (Chembridge and Spec) successfully retrieved several molecules with relatively high potency in our functional assays. The data found in Tables 4 and 5, showing the qualitative agreement between the model-derived IC_{50} values and experimentally derived functional IC_{50} values, support the predictive nature of our computational models as seen by the abilities of the pharmacophore model to retrieve promising molecules and the 3D-QSAR model to confirm inhibitory activity. The ability of the computational models to rapidly identify novel ligands should contribute significantly to drug development in this area.

The studies described here represent the first attempt to define a novel pharmacophore on $\alpha3\beta4$* nAChRs using a large number of MLA analogs. The physiochemical characterization of these noncompetitive binding sites on $\alpha3\beta4$* nAChRs should improve our understanding of the composition and functioning of nAChRs. As these studies demonstrate, application of the pharmacophore model in database mining led to the rapid identification of pharmacological activity. These data support the utility of the computational models as tools for the efficient retrieval of novel nAChR inhibitors that may lead to the identification of new therapeutic drugs that target novel sites on nAChRs.

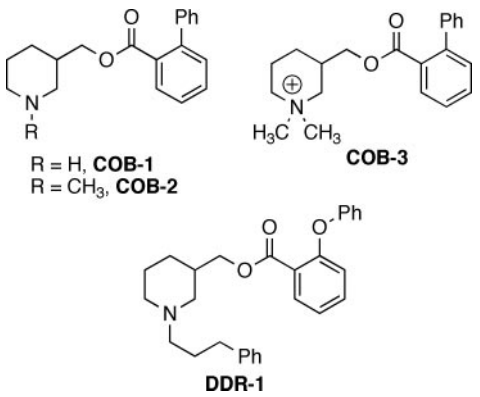

Fig. 9. Structures of compounds listed in Table 5.

References

Barker D, Lin DHS, Carland JE, Chu CPY, Chebib M, Brimble MA, Savage GP, and McLeod MD (2005) Methyllycaconitine analogues have mixed antagonist effects at nicotinic acetylcholine receptors. *Bioorg Med Chem* **13:**4565–4575.

Bergmeier SC, Ismail KA, Arason KM, McKay S, Bryant DL, and McKay DB (2004) Structure activity studies of ring E analogues of methyllycaconitine. Part 2: synthesis of antagonists to the $\alpha3\beta4$ nicotinic acetylcholine receptors through modifications to the ester. *Bioorg Med Chem Lett* **14:**3739–3742.

Bergmeier SC, Lapinsky DJ, Free RB, and McKay DB (1999) Ring E analogs of methyllycaconitine (MLA) as novel nicotinic antagonists. *Bioorg Med Chem Lett* **9:**2263–2266.

Bohacek RS and McMartin C (1992) Definition and display of steric, hydrophobic, and hydrogen-bonding properties of ligand binding sites in proteins using Lee and Richards accessible surface: validation of a high-resolution graphical tool for drug design. *J Med Chem* **35:**1671–1684.

Bryant DL, Free RB, Thomasy SM, Lapinsky DJ, Ismail KA, McKay SB, Bergmeier SC, and McKay DB (2002) Structure-activity studies with ring E analogues of methyllycaconitine on bovine adrenal $\alpha3\beta4$* nicotinic receptors. *Neurosci Res* **42:**57–63.

Clark M and Cramer RD 3rd (1993) The probability of chance correlation using partial least squares (PLS). *Quant Struct Act Relat* **12:**137–145.

Cramer RD, Patterson DE, and Bunce JD (1988) Comparative molecular field analysis (CoMFA). 1. Effect of shape on binding of steroids to carrier proteins. *J Am Chem Soc* **110:**5959–5967.

Daly JW (2005) Nicotinic agonists, antagonists, and modulators from natural sources. *Cell Mol Neurobiol* **25:**513–552.

Free RB, Bryant DL, McKay SB, Kaser DJ, and McKay DB (2002) [^{3}H]Epibatidine

binding to bovine adrenal medulla: evidence for $\alpha 3\beta 4^*$ nicotinic receptors. *Neurosci Lett* **318:**98–102.
Free RB, von Fischer ND, Boyd RT, and McKay DB (2003) Pharmacological characterization of recombinant bovine $\alpha 3\beta 4$ neuronal nicotinic receptors stably expressed in HEK 293 cells. *Neurosci Lett* **343:**180–184.
Goodall K, Barker D, and Brimble MA (2005) A review of advances in the synthesis of analogues of the delphenium alkaloid methyllycaconitine. *Synlett* **12:**1809–1827.
Gu H, Wenger BW, Lopez I, McKay SB, Boyd RT, and McKay DB (1996) Characterization and localization of adrenal nicotinic receptors: evidence that mAb35-nicotinic receptors are the principal receptors mediating adrenal catecholamine secretion. *J Neurochem* **66:**1454–1461.
Heidmann T, Oswald RE, and Changeux JP (1983) Multiple sites of action for noncompetitive blockers on acetylcholine receptor rich membrane fragments from torpedo marmorata. *Biochem* **22:**3112–3127.
Hurst T (1994) Flexible 3D searching: the directed tweak technique. *J Chem Inf Comput Sci* **34:**190–196.
Jones G, Willett P, and Glen RC (1995) A genetic algorithm for flexible molecular overlay and pharmacophore elucidation. *J Comput Aided Mol Des* **9:**532–549.
Klebe G, Abraham U, and Mietzner T (1994) Molecular similarity indices in a comparative analysis (CoMSIA) of drug molecules to correlate and predict their biological activity. *J Med Chem* **37:**4130–4146.
Kroemer RT and Hecht P (1995) Replacement of steric 6–12 potential-derived interactions energies by atom-based indicator variables in CoMFA leads to models of higher consistency. *J Comput Aided Mol Des* **9:**205–212.
Le Novere N and Changeux JP (1995) Molecular evolution of the nicotinic acetylcholine receptor: an example of multigene family in excitable cells. *J Mol Evol* **40:**155–172.
Livett BG, Gayler KR, and Khalil Z (2004) Drugs from the sea: conopeptides as potential therapeutics. *Curr Med Chem* **11:**1715–1723.
Lloyd GK and Williams M (2000) Neuronal nicotinic acetylcholine receptors as novel drug targets. *J Pharmacol Exp Ther* **292:**461–467.
Luetje CW, Wada K, Rogers S, Abramson SN, Tsuji K, Heinemann S, and Patrick J (1990) Neurotoxins distinguish between different neuronal nicotinic acetylcholine receptor subunit combinations. *J Neurochem* **55:**632–640.
Lukas RJ, Changeux J-P, le Novère N, Albuquerque EX, Balfour JK, Berg DK, Bertrand D, Chiappinelli VA, Clarke PBS, Collins AC, et al. (1999) International union of pharmacology. XX. Current status of the nomenclature for nicotinic acetylcholine receptors and their subunits. *Pharmacol Rev* **51:**397–401.
Maurer JA and McKay DB (1994) Staurosporine-induced reduction of secretory function in cultured bovine adrenal chromaffin cells. *Eur J Pharmacol* **253:**115–124.
McKay DB and Burkman AM (1993) Nicotinic and non-nicotinic receptor-mediated actions of vinblastine. *Proc Soc Exp Biol Med* **203:**372–376.
McKay DB and Sanchez AP (1990) Effect of noncompetitive nicotinic receptor blockers on catecholamine release from cultured adrenal chromaffin cells. *Pharmacology* **40:**224–230.
Olsen RW, Chang CS, Li G, Hanchar HJ, and Wallner M (2004) Fishing for allosteric sites on $GABA_A$ receptors. *Biochem Pharmacol* **68:**1675–1684.
Ward JM, Cockcroft VB, Lunt GG, Smillie FS, and Wonnacott S (1990) Methyllycaconitine: a selective probe for neuronal α-bungarotoxin binding sites. *FEBS Lett* **270:**45–48.
Xiao Y, Meyer EL, Thompson JM, Surin A, Wroblewski J, and Kellar KJ (1998) Rat $\alpha 3/\beta 4$ subtype of neuronal nicotinic acetylcholine receptor stably expressed in a transfected cell line: pharmacology of ligand binding and function. *Mol Pharmacol* **54:**322–333.
Yum L, Wolf KM, and Chiappinelli VA (1996) Nicotinic acetylcholine receptors in separate brain regions exhibit different affinities for methyllycaconitine. *Neurosci* **72:**545–555.

Address correspondence to: Dr. Dennis B. McKay, Division of Pharmacology, The Ohio State University, College of Pharmacy, 500 West 12th Avenue, Columbus, OH43210, E-mail: mckay.2@osu.edu